## Supplementary Figures

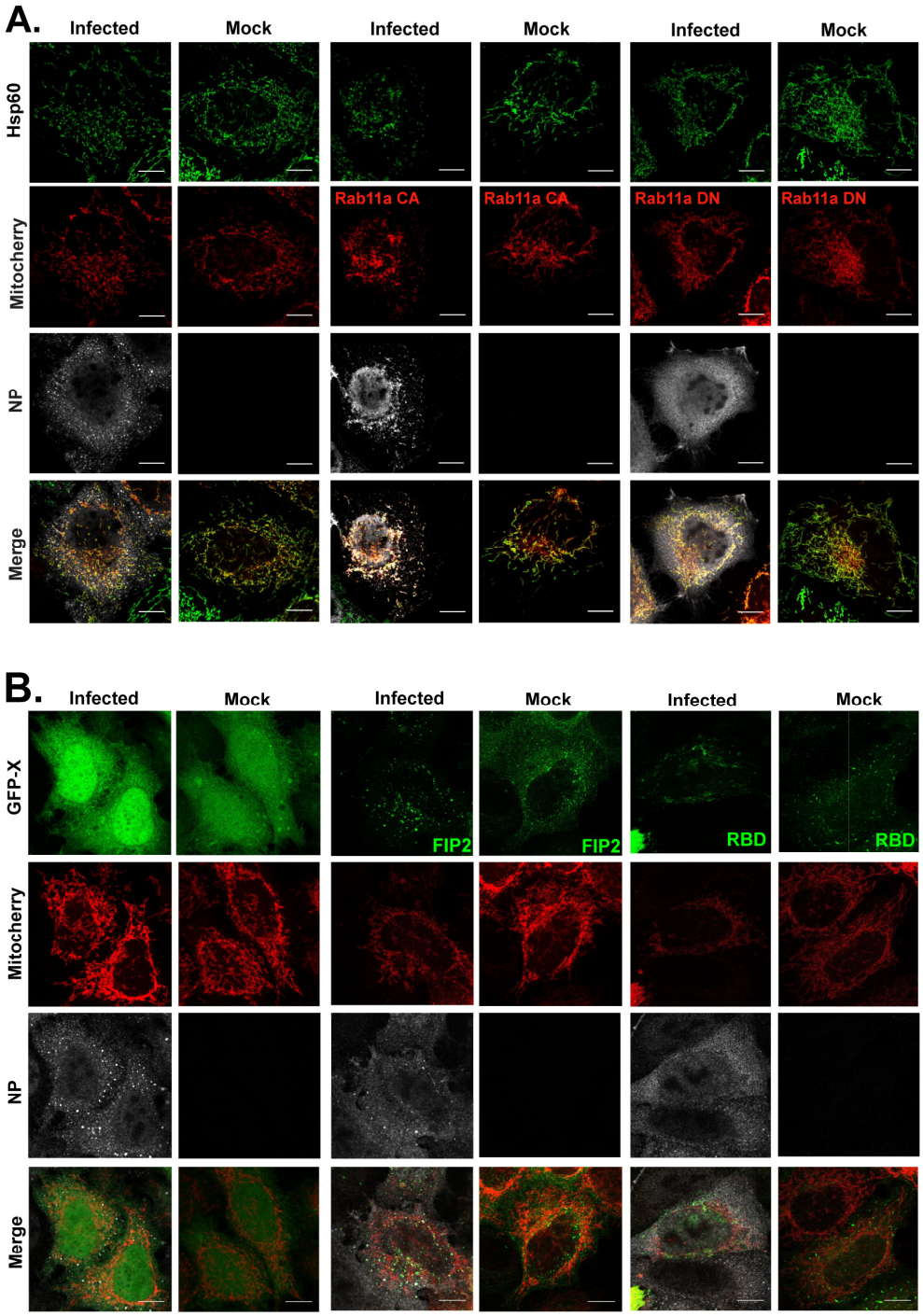


Journal of Cell Science • Supplementary information

**Figure S1 - FIPs and vRNPs compete for direct binding to mitoRab11a CA, but not mitoRab11a DN or mitocherry.**

**A.** CA and DN forms of Rab11a protein tagged with cherry at the N-terminus, or cherry only, were targeted to the mitochondria by fusion with the mitochondrial targeting sequence (MTS) of Tom20 (=mitoRab11a CA / mitoRab11 DN / mitocherry). HeLa cells were transfected with these three plasmids individually and infected with PR8 at MOI 20. At 14h p.i., cells were fixed and processed for immunofluorescence staining of Hsp60 and/or viral NP. **B.** HeLa cells were co-transfected with mitocherry and either GFP alone (X=-) or GFP-X (X=FIPs) and sequentially infected or mock-infected with PR8 at MOI 20. At 14h p.i., cells were fixed and processed for immunofluorescence staining of viral NP. Bar=10 μm. Images are representative of two independent experiments. An average of 30 cells was analyzed per condition per experiment.

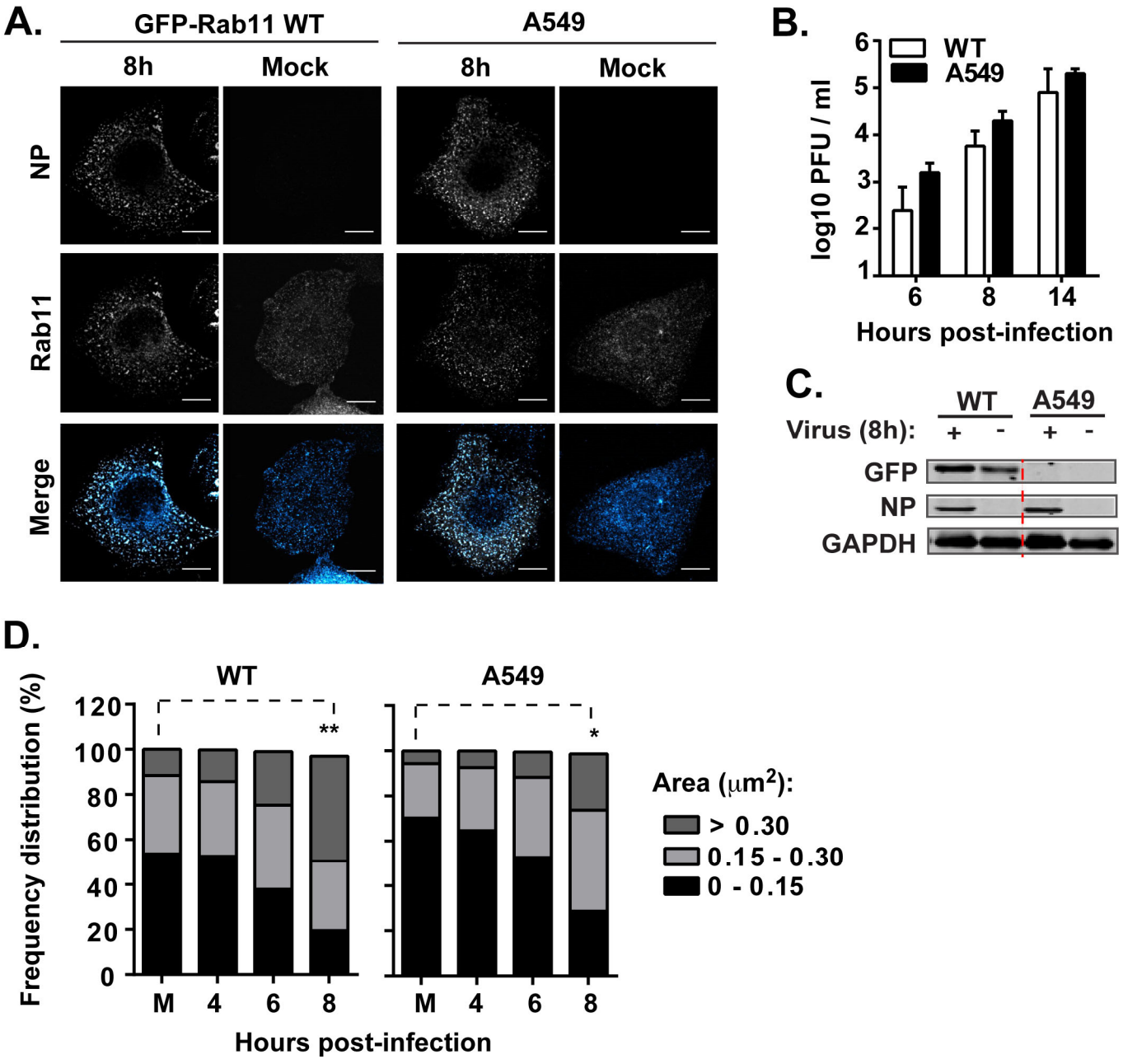


**Figure S2 - Cells stably overexpressing GFP-Rab11a behave similarly to cells expressing endogenous levels of Rab11a.**

A549 cells alone or stably overexpressing GFP-Rab11a WT were infected or mock (M)-infected with PR8 at MOI 3. At the indicated time points: **A.** Cells were fixed and processed for immunofluorescence staining of Rab11 and viral NP. Bar=10 μm. **B.** Viral titres were quantified by

plaque formation on MDCK cells and expressed as the logarithm 10 of plaque forming units (PFU) per ml ± SEM. Statistical analysis of data was performed using two-way ANOVA, followed by a Dunnett's multiple comparisons test (no significant differences detected). **C.** GFP-tagged proteins, viral NP and GAPDH levels were detected by Western blot. **D.** The frequency distributions (%) of small, medium and large Rab11-vesicle areas ($\mu m^2$) were plotted over the course of infection. Statistical analysis of data was performed using a two-way ANOVA test, followed by Tukey's multiple comparisons test (*$p<0.05$; **$p<0.01$). Experiments were performed twice and an average of 30 cells per experiment were analysed.

**Chart showing procedure for the acquision of EM and confocal images**

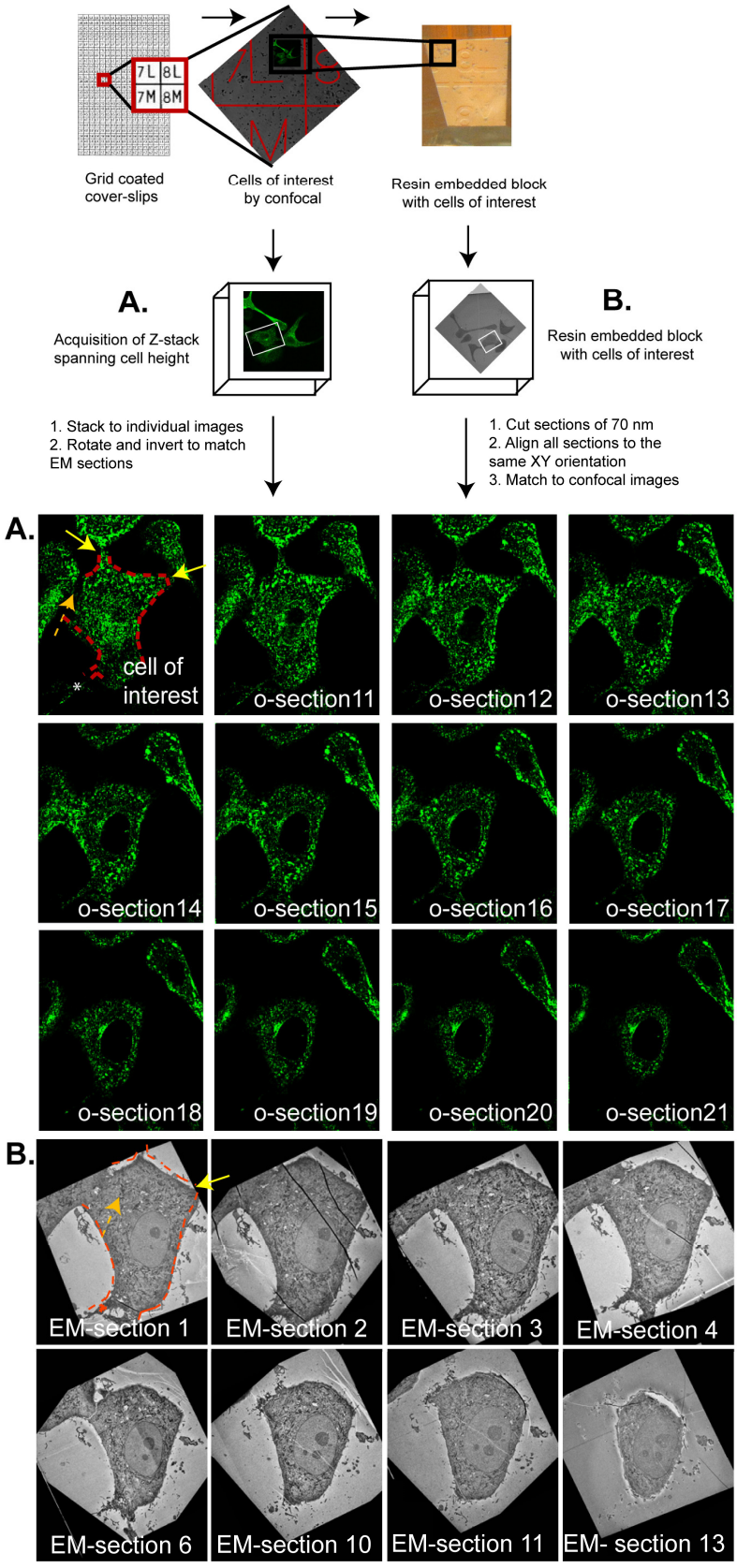

**Figure S3 - Strategy to acquire images of cells of interest by confocal and electron microscopy images.**

A549 cells stably expressing GFP-Rab11a were grown on gridded coverslips, infected with PR8 at a MOI of 3. **A.** Cells were fixed and imaged for confocal microscopy to acquire Z-stacks of the cells of interest. **B.** Cells were then processed for electron microscopy (EM), serial sectioned at 70 nm and imaged using the electron microscope, throughout the whole depth of the cell. **A. B.** Images spanning the entire volume of the cell from confocal (o-section) and EM (EM-section) were observed to make correspondence between the two methods. Cell shape, cell-to-cell contacts (see arrows) and cell holes (see asterisk in the first confocal image and EM section 1) were taken into consideration to match confocal and EM serial sections.

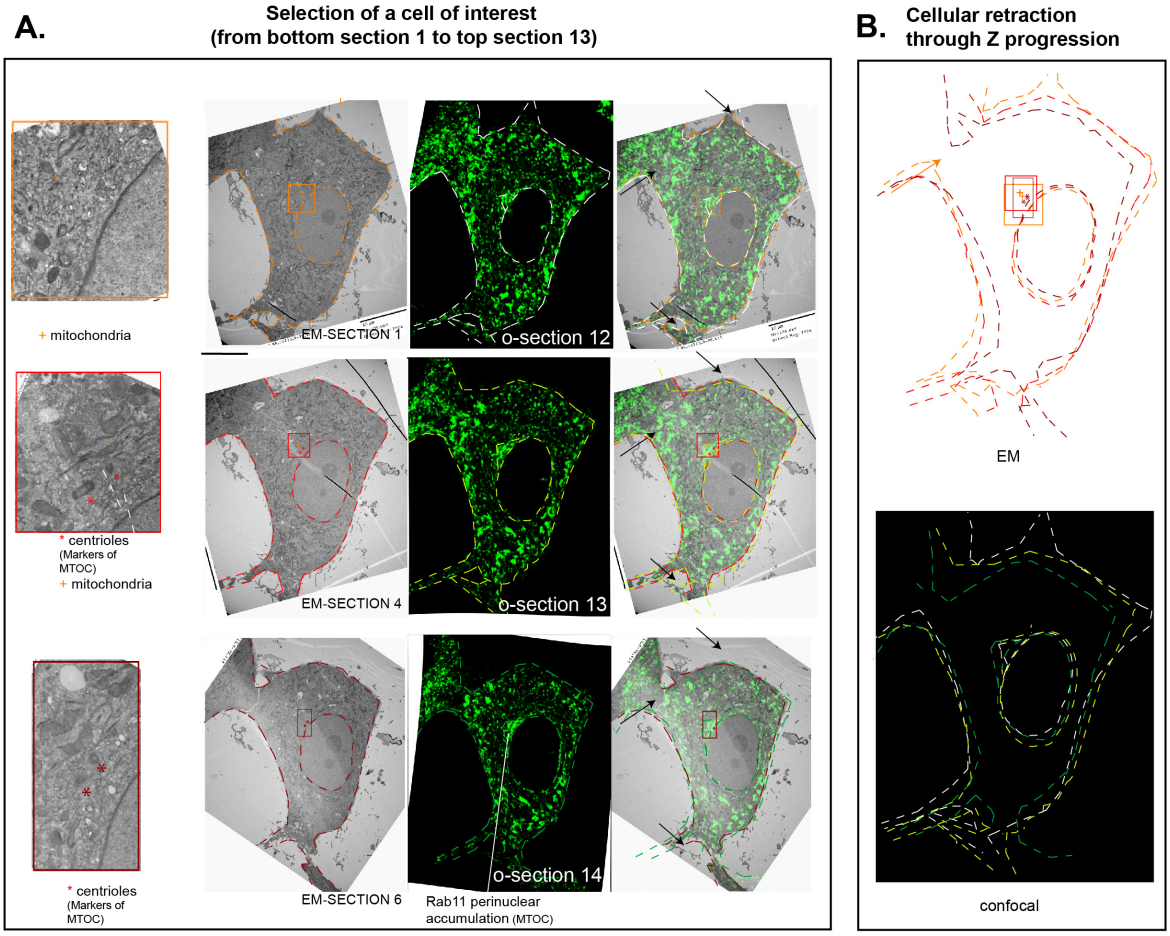


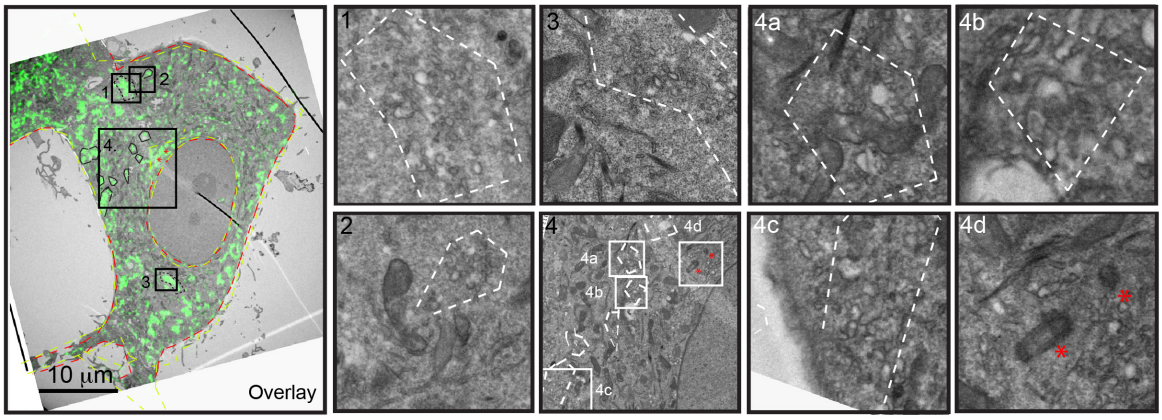


**Figure S4 - Strategy to refine alignment between confocal and EM images.**

**A.** Matching between confocal and EM images was refined using structural features that include: cell-to-cell contacts (arrows) that are established or lost when moving away the basal side; centrioles as markers of the microtubule organizing center (MTOC) in EM and Rab11 accumulation

in the same region by confocal; nuclei size, cell holes (see asterisk in the first confocal image and EM section 1). **B.** Parameters evaluated to confirm alignment included cell shape variation during Z-stack progression by EM (top) and confocal imaging (bottom) between serial sections. **C.** Example of a final figure containing ultrastructural details from the Overlay image. The Overlay image corresponds to a section in the confocal and EM matched as explained in Figure S6 and S7A. The detailed regions were obtained by delineating the green areas in the Overlay with dashed lines, and drawing a square around the area to be magnified. These marks were amplified to fit the edges of EM figures of higher magnification without any distortions. The process was repeated to further amplify areas of interest that resulted in series 4a-d. Features like the MTOC, easily detected in both systems validated the alignment. For this, we used the described Rab11 accumulation at the perinuclear region surrounding the MTOC observable by confocal to successfully predict the location of the centrioles in EM images (red asterisks in 4d).